# Mechanical and Thermal Properties of Eva Blended with Biodegradable Ethyl Cellulose

**B. G. Girija,[1] R. R. N. Sailaja,[2] Sharmistha Biswas,[2] M. V. Deepthi[2]**

[1]*Department of Chemical Engineering, Indian Institute of Science, Bangalore 560012, India*
[2]*The Energy and Resources Institute (TERI), Southern Regional Centre, Bangalore 560071, India*

Received 6 June 2008; accepted 26 September 2009
DOI 10.1002/app.31660
Published online 17 December 2009 in Wiley InterScience (www.interscience.wiley.com).

**ABSTRACT:** In this study, biodegradable blend of Poly (Ethylene-*co*-Vinyl Acetate) (EVA) and Ethyl Cellulose (EC) were prepared. Ethylene vinyl alcohol (EVOH) copolymer was used as an interfacial compatibilizer to enhance adhesion between EVA and EC. The melt blended compatibilized biocomposites were examined for mechanical and thermal properties as per the ASTM standards. It has been found that the EC has a reinforcing effect on EVA leading to enhanced tensile strength and also impart biodegradability. Thus, a high loading of 50% EC could be added without compromising much on the mechanical properties. Analysis of the tensile data using predictive theories showed an enhanced interaction of the dispersed phase (EC) and the matrix (EVA). The compatibilizing effects of EVOH on these blends were confirmed by the significant improvement in the mechanical properties comparable with neat EVA as also observed by SEM microscopy. The TGA thermograms exhibits two-stage degradation and as EC content increases, the onset temperature for thermal degradation reduces. © 2009 Wiley Periodicals, Inc. J Appl Polym Sci 116: 1044–1056, 2010

**Key words:** EVA; ethyl cellulose; compatibilizer; mechanical and thermal properties; biodegradation

## INTRODUCTION

Biobased-plastics are gaining prominence owing to their biodegradability and eco-friendly characteristics. This would also reduce our dependence on the depleting petroleum reserves. Microbial plastics like polyhydroxyalkanoates (PHA), polyhydroxy butyrate (PHB), etc. are expensive. Another alternative is to blend the synthetic polymers with inexpensive biopolymers. Among the various plastics, polyolefins have the largest tonnage in the world. EVA is one such polyolefin which is widely used in packaging, footwear, cables, agricultural mulch films, etc. Thus, disposal of EVA in the postconsumer waste is essential owing to growing environmental concerns. Mothe and Tavares[1] examined the thermal stability and biodegradability of polysaccharide-blended EVA from shoe rejects. Starch-based biodegradable films were developed as alternative to commercial agricultural EVA and LDPE plastic films. It was suggested that such biobased films would ensure landscape protection from pollution.[2] Testing of biodegradable mulch films with the conventionally used PE/EVA films under real field conditions showed improved performance accompanied by biodegradability properties.[3] Biodegradable EVA foams comprising of powdered grain husks and wood shavings were developed by Shyu and Shyu.[4] A biodegradable composite of starch/EVA reinforced with coir was prepared by Rosa et al.[5] Mercerized fibers gave better mechanical properties than untreated fibers. A blend of PHB with EVA was prepared by Kim et al.[6] It was found that very high content of EVA was detrimental to the biodegradability of PHB. These blends also exhibited phase separation owing to poor adhesion between the phases.[7] Blends of EVA with Polyvinyl acetate were tested for degradability by Rimez et al.[8] Biodegradable blends of EVA with PLA exhibited poor mechanical properties owing to their immiscibility.[9] EVA/Cellulose composites were studied for structure-properties relations by Gregory et al.[10] A detailed study of interfacial interactions was analyzed. Pyrolytic decomposition kinetics of EVA/Cellulose mixtures revealed slight lowering of degradation temperature when compared with neat polymer.[11] To improve adhesion between the two phases, EVA was used as compatibilizer.[12,13] EVA compatibilized biodegradable starch-based composites were prepared by Senna et al.[14] It was found that electron beam irradiation further improved the compatibility of the blends. EVA/Sisal fiber grafted composites showed good interfacial adhesions when compared with unmodified composites.[15] The biodegradable component should exhibit good adhesion

*Correspondence to:* R. R. N. Sailaja (rrnsb19@rediffmail.com).

Contract grant sponsors: Department of Science and Technology (DST).

with the other phase so as to ensure high filler loadings with comparable mechanical properties as the matrix polymer. In this study, ethyl cellulose has been thus chosen as the biodegradable component. Ethyl Cellulose (EC) is a hydrophobic cellulose derivative with rigid main chains unlike hydrophilic starch or cellulose. Similar biodegradable blends using EC/Polycaprolactone (PCL) and Polylactic acid (PLA)/EC blends have been prepared by Yiking et al.[16] and Wu et al.[17] Miscible blends of PHB/EC blends were prepared to produce cost effective bioplastics.[18] In this study, EVA has been blended with EC using EVOH as the interfacial agent. The mechanical and thermal properties of the blend have been examined for EC loadings up to 60%. Addition of compatibilizer to this blend slightly improves the impact and tensile strength for 20–40% EC loadings. The blends exhibit an optimum at 6% compatibilizer. No such studies have been found in the literature so far.

## EXPERIMENTAL

### Materials

The poly (ethylene-*co*-vinyl alcohol) (EVOH) copolymer was obtained by the hydrolysis of an ethylene vinyl acetate copolymer (EVA) (from NOCIL, Mumbai, India) of 43% (by weight) vinyl acetate content. The degree of hydrolysis was measured to be 89% as done earlier by Sailaja and Chanda.[13] Ethyl cellulose (EC) powder was obtained from Sigma Aldrich (USA). All other solvents were obtained from S.d. Fine Chem (Mumbai).

### Blend preparation

Blends of EVA, EC, and EVOH were prepared by melt mixing at 210°C in a locally fabricated kinetic mixer where small quantities can be used. In all blends, the content of EC was varied from 0 to 60%. Furthermore, the compatibilizer content was varied for 0 to 15% of the filler weight. The amount of compatibilizer (EVOH) added is expressed as the weight percent of filler (EC). Dumb-bell shaped specimens were then molded as per ASTM specifications into standard dies supplied with the Minimax molder (Custom Scientific Instruments, New Jersey, Model CS-83MMX). These dumb-bell specimens were then subjected to impact and tensile tests using Minimax testing units.

### Mechanical properties of the blend

A Minimax impact (Model CS-83T1079) and tensile tester (model CS-83TTE, Custom Scientific Instruments, NJ) was used to measure (unnotched) impact strength (RIS) and tensile properties, respectively. The values obtained for the blends of EVA has been compared with the values of pure EVA as relative impact strength (RIS) (i.e., ratio of the impact strength of the blend to impact strength of neat EVA), relative tensile strength (RTS), relative Young's modulus (RYM), and relative elongation at break (REB). At least, eight specimens were tested for each variation in the composition of the blend. The impact and tensile tests were performed as per ASTM D1822 and ASTM D1708 methods, respectively. The strain rate used for all tensile measurements were made at a bar speed of 10 mm/min throughout the study.

### Thermal analysis

Thermogravimetric analysis (TGA) was carried out for the EVA as well as for the blends using Perkin-Elmer Pyris Diamond 6000 analyzer in nitrogen atmosphere. The sample was subjected to a heating rate of 10°C/min in the heating range of 40–600°C using $Al_2O_3$ as the reference material.

### Blend morphology

Scanning electron microscope (SEM) (JEOL, JSM-840A) was used to study the morphology of fractured and unfractured specimens. The specimens were gold sputtered before microscopy (JEOL, SM-1100E). The morphology of the unfractured blend specimens was taken after soaking the samples for 2 h in sulfuric acid at room temperature. Sulfuric acid was used for etching out the EC phase of the blend.

## RESULTS AND DISCUSSIONS

Biodegradable blends of EVA and ethyl cellulose have been prepared. EVOH has been added to compatibilize the two phases. The thermal, mechanical, and morphological studies for these blends have been conducted. Statistical analysis of the mechanical properties has been carried out using Sigma plot software (Version 2000). To determine the quantitative relationship between response (F) (e.g., RIS) and the system variables, i.e., compatibilizer percentage ($x$) and filler content ($y$), the experimental data was fitted with the quadratic equation represented by eq. (1).

$$F = a_0 + a_1x + a_2y + a_3x^2 + a_4y^2 + a_5xy + a_6x^2y + a_7xy^2 \quad (1)$$

The values of coefficients ($a_1$–$a_7$) of the fitted eq. (1) are given in Table I. The $\langle r^2 \rangle$ value for the earlier equation has been greater than 0.8 and this suggests

**TABLE I**
**List of Coefficients for eq. (1)**

| Property ($F$) | Residual ($R^2$) | Standard error of estimate | Linear terms | | | Quadratic terms | | Interaction terms | | |
|---|---|---|---|---|---|---|---|---|---|---|
| | | | $a_0$ | $a_1$ | $a_2$ | $a_3$ | $a_4$ | $a_5$ | $a_6$ | $a_7$ |
| RIS | 0.94 | 0.0650 | 0.64 | 5.70 | 1.04 | −77.65 | −3.58 | −25.45 | 102.37 | 33.57 |
| RTS | 0.93 | 0.0789 | 1.43 | 1.16 | −3.99 | 283.62 | 6.19 | −31.18 | −1066.68 | 135.26 |
| RYM | 0.88 | 0.1487 | −0.09 | 48.53 | 10.30 | 683.42 | −11.9 | −500.83 | −1045.37 | 731.73 |
| REB | 0.81 | 0.1374 | 0.74 | 21.62 | −0.47 | −266.42 | −1.27 | −66.46 | 514.18 | 45.05 |

that the earlier equation gives good prediction for the obtained experimental results.

## Blend morphology

Figure 1 shows the blend morphology of EVA/EC blends. The blend specimens were soaked in sulfuric acid for 3 h. The sample specimens were then washed thoroughly with distilled water and dried. Figure 1(a) shows a deformed matrix with a large patches of elongated large voids and small voids for 40% EC loading (uncompatibilized blend). The compatibilized counterpart shown in Figure 1(b) exhibits a highly interlocked surface in combination with a large number of elongated voids. The elongated voids indicated debonding of particles from the matrix and the interlocking of matrix is due to the resistance offered by the matrix for the particle removal during etching. This suggests that there are strong interactions between EVA and EC.

Figure 1(c,d) exhibits the surface morphology of EVA/EC blends with 60% EC loading. The uncompatibilized blend shown in Figure 1(c) shows a deformed matrix with large holes which occurred due to the debonding of agglomerated particles. However, it is interesting to observe that there is some adhesion between and matrix and filler even at such high EC loading. The compatibilized blend [Fig. 1(d)] exhibits an interlocked surface owing to enhanced interaction between the two components.

The carbonyl group of EVA can react with ethyl cellulose leading to interfacial reactions. The addition of compatibilizer further enhances the interactions of the ester groups (of EVA) and ether groups

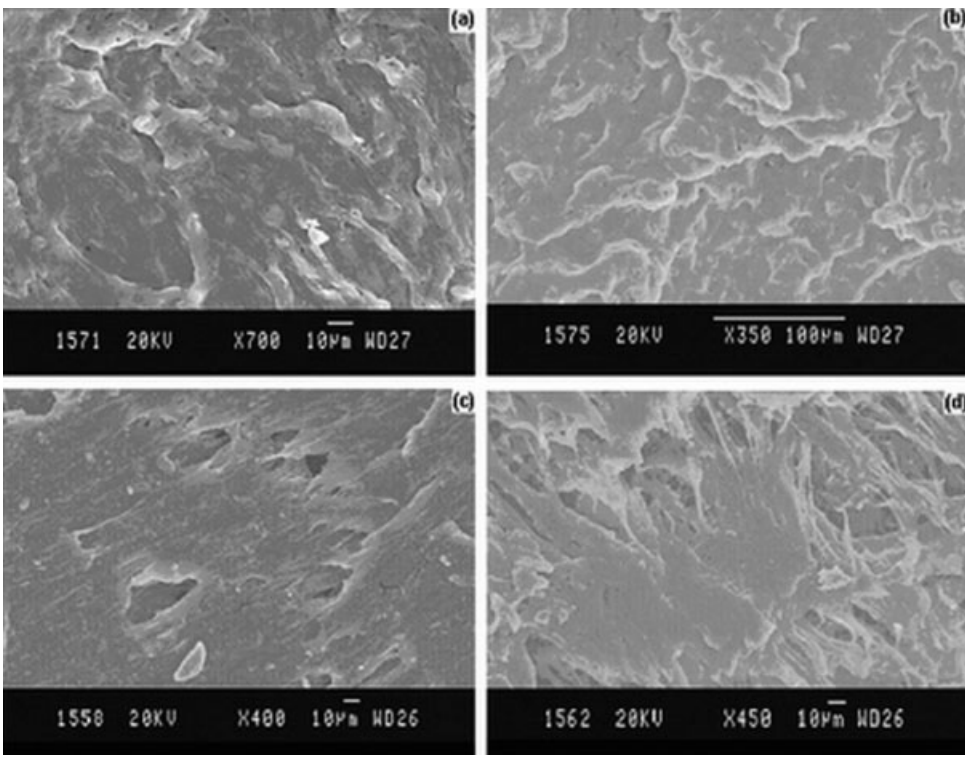


**Figure 1** SEM micrographs showing blend morphology (a) blend containing 40% EC and no compatibilizer; (b) blend containing 40% EC and 6% compatibilizer; (c) blend containing 60% EC and no compatibilizer; and (d) blend containing 60% EC and 6% compatibilizer.

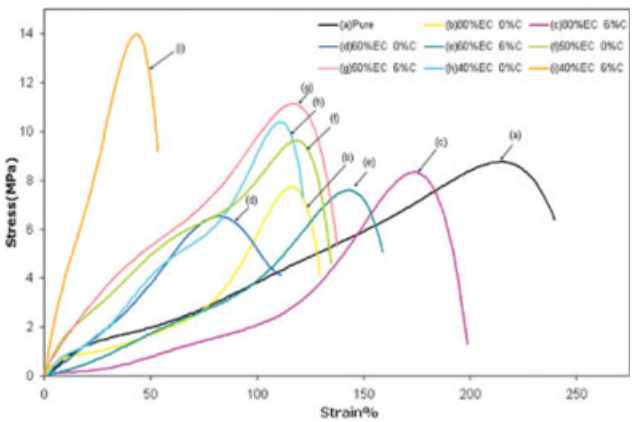


**Figure 2** Stress/Strain curves for EVA/EC blends. [Color figure can be viewed in the online issue, which is available at www.interscience.wiley.com.]

(of EC) with the hydroxyl groups of EVOH thereby, leading to improved properties. The uncompatibilized blends also exhibits high-tensile strength owing to the compression extended by the crystalline matrix on the semicrystalline matrix on the semicrystalline filler leading to good interfacial contact.[19]

### Stress–strain curves

Figure 2 shows the engineering stress–strain curves for EVA/EC blends. Curves (b) and (c) show, respectively, the uncompatibilized and compatibilized stress–strain properties for 20% EC loading. The curve (c) shows higher stress yielding when compared with curve (b). For 40% EC loading [curve (d)] shows lower stress yielding when compared with that obtained for 20% loading. The compatibilized counterpart [curve (e)] shows a higher stress value than the uncompatibilized blend. As the EC loading increases the stress yielding occurs at higher value but the specimen fractures just after yielding. This results as EC chains are rigid resulting in higher yield strength. However, all specimens exhibit lower strain values when compared with neat EVA (curve (a)). For 60% EC loading [curve (f)], blend shows high-tensile strength but poor ductility. As EC particles are rigid by nature, they do not undergo elongation. At such a high loading of 60% EC, the blend may have undergone phase inversion and as the EVA content is less than EC, the composite behaves like a rigid material. The 6% compatibilization [curve (g)] slightly improves the strain values. However, the compatibilized blends also exhibit brittle characteristics.

### Effect of compatibilizer

The blends EVA and EC have been mixed using EVOH as compatibilizer. It is obvious that EVOH is able to anchor the EVA and EC effectively as EVOH has both the ethylene repeating units and the hydroxyl groups which can hold the two immiscible phases together. Furthermore, Figure 2 shows the effect of compatibilizer on different mechanical properties.

Figure 3(a) shows the effect of percentage compatibilizer and RIS (i.e., impact strength of the blend/impact strength of pure EVA). Addition of compatibilizer improves the impact strength for 20–40% EC loading. However, for EC loadings of 50% and 60% the impact strength of compatibilized blends increases by 60% when compared with uncompatibilized blends. Figure 3(b) shows the effect of adding compatibilizer on RTS. The tensile strength of uncompatibilized blends does not reduce indicating that there is some affinity between ethyl cellulose (EC) and EVA. Addition of compatibilizer to this blend slightly improves the tensile strength for 20–40% EC loadings. For 50% and 60% EC loading, there is a significant improvement in RTS and the blend exhibit an optimum at 6% compatibilizer. Increasing the compatibilizer content beyond 6% is detrimental to the blend properties. This may be because of the saturation of reactive sites at the blend interfaces. Such a phenomenon has been reported by Lomellini et al.[20] and Sundararaj and Macosko.[21] It has been observed that higher concentration of the compatibilizer content does not lead to a significant decrease of the interfacial tension; therefore, it becomes progressively more difficult for the compatibilizer chains to go to the interface, and it will remain randomly entrapped in one of the phases. Figure 3(c) shows the RYM versus percentage compatibilizer for EVA–EC blends. The uncompatibilized blends exhibit higher RYM values than neat EVA, whereas the compatibilized blends have lowered modulus values. As the compatibilizer content increases the RYM values approach those of neat EVA due to enhanced interaction due to reactive compatibilization. Figure 3(d) shows the variation of REB values on compatibilizer addition for these blends. For 20–40% EC loadings, compatibilizer improves the REB values exhibiting an optimum at 9% compatibilizer content. For higher loadings of 50% and 60% EC, there is no improvement in REB values, inspite of compatibilization. The rigid ethyl cellulose chains impart brittleness to the blend.

The blend properties are higher for the compatibilized blends except for modulus values when compared with those obtained with 0% compatibilizer. EVOH acts as a compatibilizer and has been able to anchor efficiently with the two immiscible phase. In all cases, optimum compatibilizer content is observed for the blends. This suggests that the compatibilizer behaves like a third phase rather than an anchoring agent beyond the optimal compatibilizer

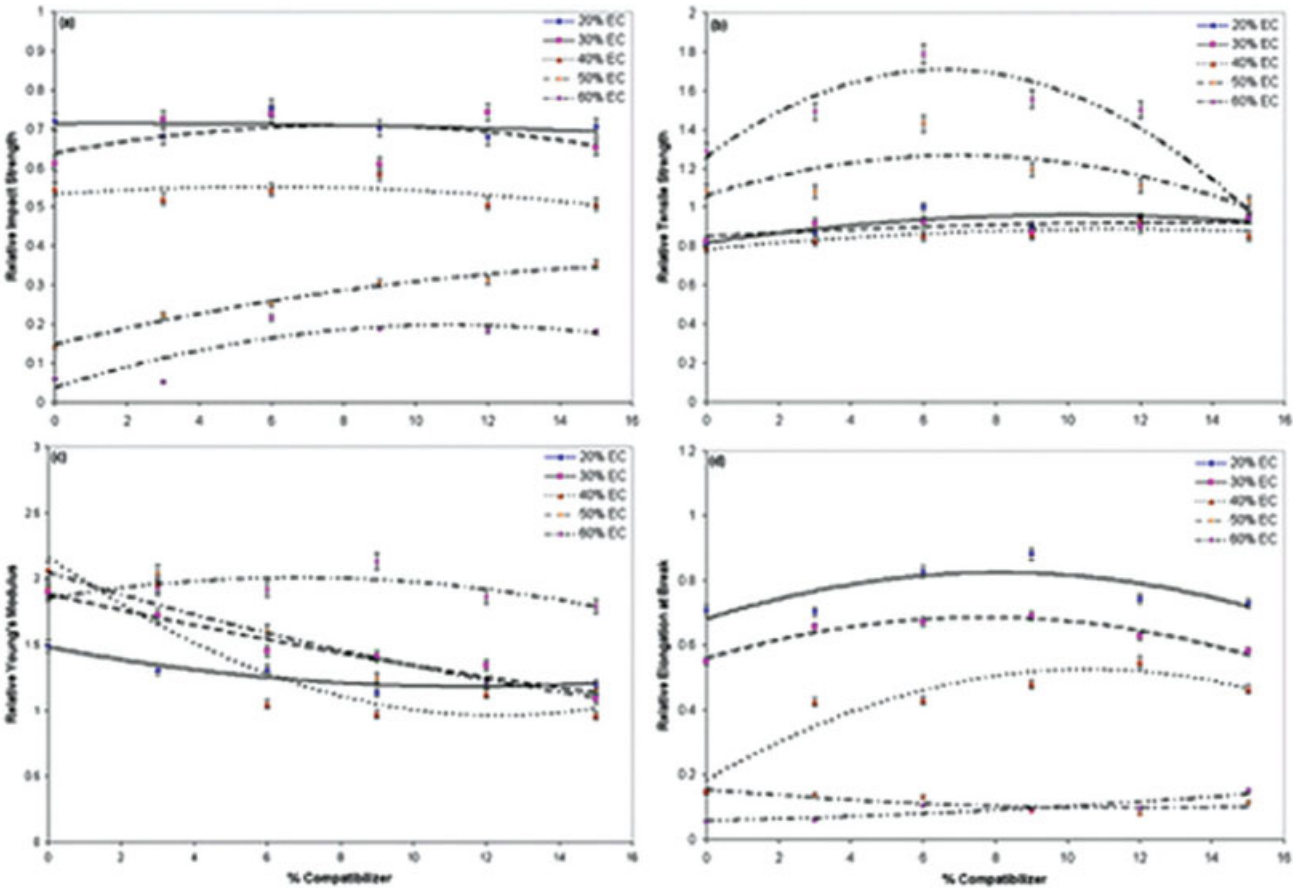


**Figure 3** Plot of effect of Compatibilizer on the mechanical properties for EVA/EC blends (a) RIS versus percentage compatibilizer for the blends; (b) RTS versus percentage compatibilizer for the blends; (c) RYM versus percentage compatibilizer for the blends; and (d) REB versus percentage compatibilizer for the blends. [Color figure can be viewed in the online issue, which is available at www.interscience.wiley.com.]

loading. Thus, this is a case of reactive blending between the ether and unsubstituted groups of EC and the hydroxyl groups of EVOH. A similar observation of the reaction between ether and hydroxyl groups has been found by Yamaoka and Watanabe.[22]

Apart from this, the ester group of EVA interacts with the ether and hydroxyl group of EC. A similar case of reactive blending between EC and polymethyl methacrylate has been carried out by Datt et al.[23] and Giunchedi et al.[24] Thus, even for uncompatibilized blends, the RTS values are almost 60% or above for uncompatibilized blends [Fig. 3(a)] even for 40% EC loading. Similar interactions between acetylated starch and EVOH blends have been found by Jiang et al.[25]

### Effect of filler loading

#### Relative impact strength

Figure 4 shows the RIS versus volume fraction of ethyl cellulose filler with varying compatibilizer content.

The volume fraction of the filler ($\phi_f$) has been calculated using the following eq. (2).

$$\phi_f = \frac{W_i/\rho_i}{\Sigma W_i/\rho_i} \tag{2}$$

In eq. (2), $W_i$ and $\rho_i$ is the weight fraction and density of component $i$ in the blend, respectively. The density values of EVA, EC, and EVOH has been taken 0.939 g/cm$^3$, 1.13 g/cm$^3$, and 1.14 g/cm$^3$, respectively. The RIS values reduces as filler volume fraction increases as shown in Figure 4(a–f). For 20–40% filler addition, compatibilization slightly improves the impact strength values. For 20% and 30%, the impact strength of the blend is around 74% of that of neat EVA. For higher, i.e., 40% EC loading, the RIS value is around 0.6, i.e., 60% of that of neat EVA and for EC loadings of 50% and above, the impact strength is only 30% of that of neat EVA even with compatibilizer.

The SEM micrographs of the impact fractured specimens are shown in Figure 5(a–d). Figure 5(a) shows the impact fractured surface of 20% EC-filled

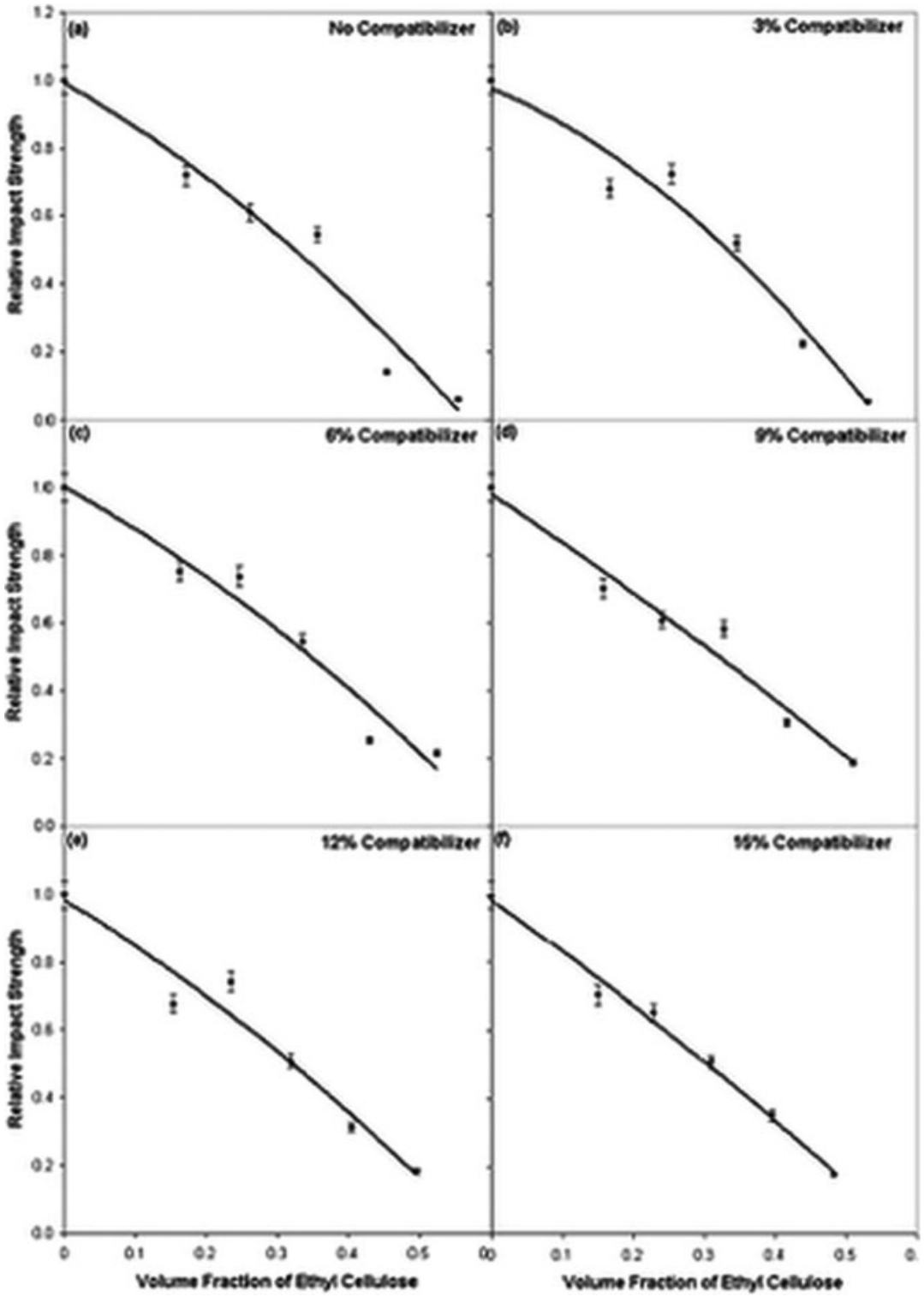


**Figure 4** Variation of RIS with volume fraction of EC for (a) no compatibilizer; (b) 3% compatibilizer; (c) 6% compatibilizer; (d) 9% compatibilizer; (e) 12% compatibilizer; and (f) 15% compatibilizer.

uncompatibilized composite. The micrograph exhibits ductile fracture characteristics. The SEM micrograph exhibits extensive crazing accompanied by severe deformation of the matrix. The voids left by the cavitation of the EC particles are also seen in the micrograph. This is also reflected in the high RIS value (0.72). Both EVA and EC are polar and hydrophobic in nature and blend thus exhibits adhesion to a certain extent.

The compatibilized (6% compatibilizer) counterpart also exhibits similar fracture surface characteristics. This is also reflected in the RIS value as the

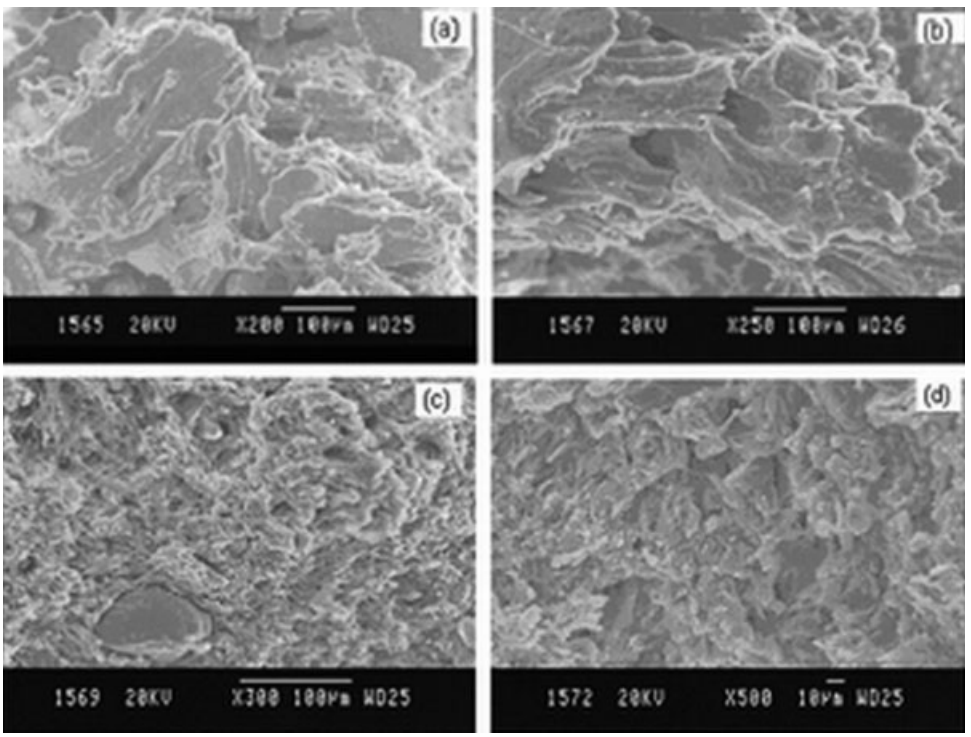


**Figure 5** SEM photographs showing impact fractured blend specimens (a) blend containing 20% EC and no compatibilizer; (b) blend containing 20% EC and 6% compatibilizer; (c) blend containing 40% EC and no compatibilizer; and (d) blend containing 40% EC and 6% compatibilizer.

increase is only nominal (0.75). Figure 5(c) shows the impact fracture surface of uncompatibilized EVA–EC blend with 50% EC loading. The SEM micrograph is typical of brittle fracture along with cavitation of EC. The compatibilized blend [Fig. 5(d)] also shows brittle nature accompanied by slight shearing of the EVA matrix indicating enhanced interactions. This improvement of impact strength values in the compatibilized blend is also reflected by an enhanced value of impact strength to around 22% when compared with uncompatibilized blends.

## Relative tensile strength

Figure 6 shows the RTS versus volume fraction of EC for various compatibilizer loadings. The RTS values reduce as the volume fraction increases up to 40% EC content. For 50% and 60%, RTS values are more than 1.0 even without compatibilizer. This may be due to phase inversion or the blend has cocontinuous morphologies. More studies on this aspect are required and are beyond the scope of this work [Fig. 6(a)]. Figure 6(b–d) show improvement in RTS values up to 6% compatibilizer addition and RTS values are more than 1.8. Higher compatibilizer levels beyond 6% do not contribute to the improvement in tensile strength.

Three theoretical models have been used to predict the tensile strength of EVA/EC blends. The first is the Nicolais and Narkis model[26] given as follows.

$$\mathrm{RTS} = \frac{\sigma_b}{\sigma_{\mathrm{EVA}}} = 1 - 1.21\phi_f^{2/3} \tag{3}$$

In the earlier equation, $\sigma_b$ and $\sigma_{\mathrm{EVA}}$ is the tensile strength of the blend and tensile strength of neat EVA, respectively. The value of tensile strength of pure EVA ($\sigma_{\mathrm{EVA}}$) obtained was 8.05 MPa. The $\langle r^2 \rangle$ value for the earlier eq. (3) is given in Table II. This model assumes no adhesion between filler and matrix. Hence, in Figure 6, the results of this model do not match at all with the experimental result which indicates that strong interactions exist between EVA and EC.

The second model is the Halpin-Tsai model[27] and is given by,

$$\mathrm{RTS} = \frac{\sigma_b}{\sigma_{\mathrm{EVA}}} = \frac{1 + G\eta_T\phi_f}{1 - \eta_T\phi_f} \tag{4}$$

where, $\eta_T$ is given by,

$$\eta_T = \frac{R_T - 1}{R_T + G} \tag{5}$$

where, $R_T$ is the ratio of filler tensile strength to that of neat EVA. $G$ is a constant given in eq. (6) below as follows [eq. (6)]

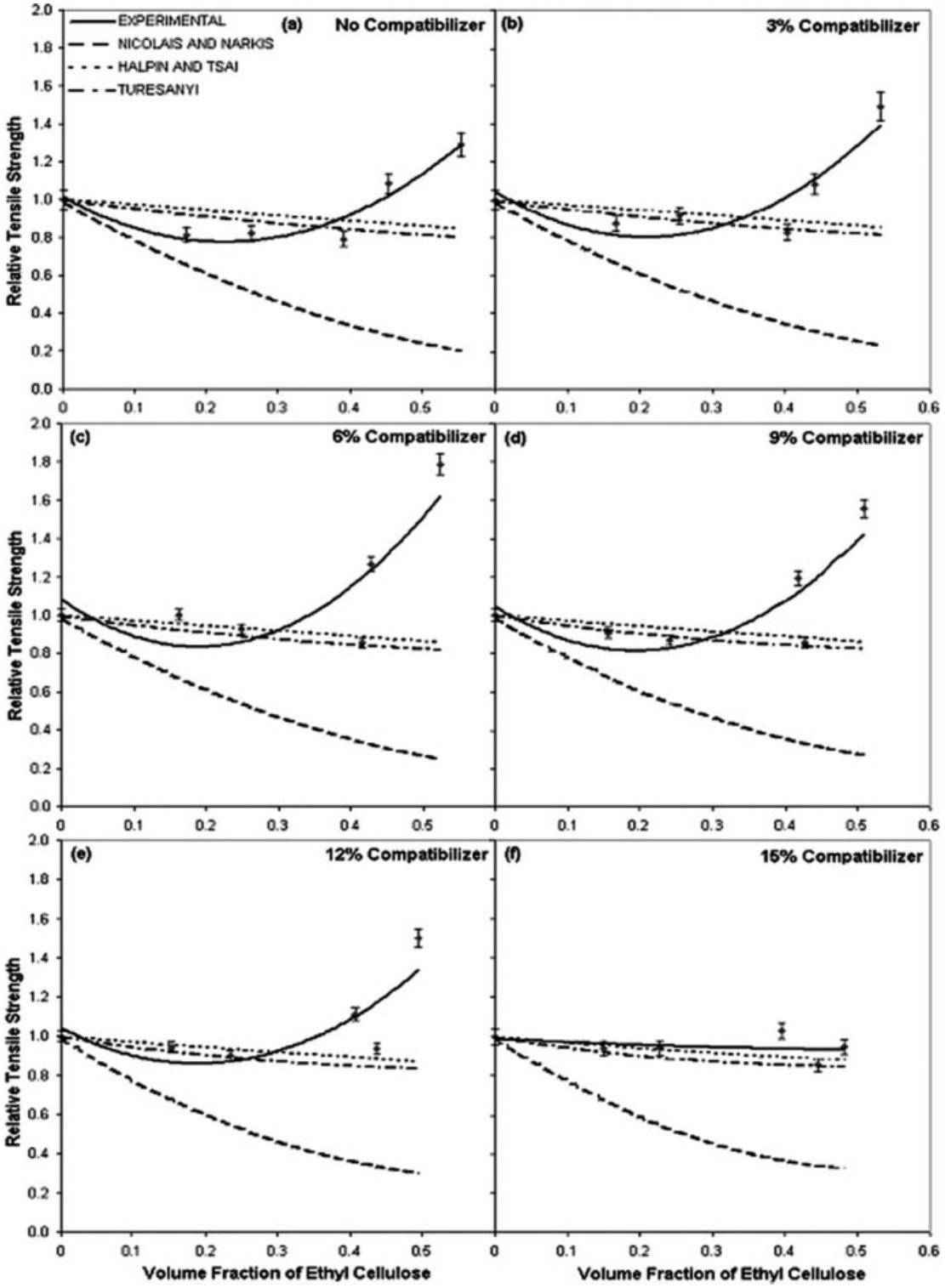


**Figure 6** Variation of RTS with volume fraction of EC for (a) no compatibilizer; (b) 3% compatibilizer; (c) 6% compatibilizer; (d) 9% compatibilizer; (e) 12% compatibilizer; and (f) 15% compatibilizer.

$$G = \frac{7 - 5\upsilon}{8 - 10\upsilon} \tag{6}$$

In eq. (6), $\upsilon$ is the Poisson's ratio of neat EVA and is taken to be 0.49.[28] $R_T$ value was found by trial and error to match the experimental results and this was found to be 0.73. The theoretical results from this model are also plotted in Figure 5. The $\langle r^2 \rangle$ value for the above eq. (4) is given in Table II. The experimental results are closer to the predicted results when compared with those predicted by Nicolais and Narkis [eq. (3)]. The model assumes

**TABLE II**
**List of $\langle r^2 \rangle$ Values for all Theoretical Models**

| | Property (*F*) | | | | | | |
|---|---|---|---|---|---|---|---|
| | RTS | | | RYM | | | REB |
| | Nicolais-Narkis | Halpin-Tsai | Turcsanyi | Kerner | Halpin-Tsai | Sato-Furukawa | Neilsen |
| Residual $\langle r^2 \rangle$ | 0.97 | 0.96 | 0.95 | 0.99 | 0.99 | 0.99 | 0.98 |

perfect adhesion between filler and matrix. As the experimental values are closer to those obtained using eq. (4), the results indicates certain degree of adhesion.

The third model is the Turcsanyi model[29] and is described by the following eq. (7) given below.

$$\mathrm{RTS} = \frac{\sigma_b}{\sigma_{\mathrm{EVA}}} = \frac{1 - \phi_f}{1 + 2.5\phi_f} \exp(B\phi_f) \qquad (7)$$

In the earlier eq. (7), $B$ is a parameter which depends on interfacial adhesion. For poor adhesion, the $B$ value is less than 1.0 and as the interfacial adhesion improves, the value exceeds 1.0.[29] The $\langle r^2 \rangle$ value for the earlier eq. (7) is given in Table II. For the EVA/EC blends, the value of $B$ has been found to be 2.6. This indicates that there is an efficient stress transfer from matrix to filler during tensile rupture. Figure 6 also shows that the theoretical values from this model match closely with the experimental results. Thus, the obtained experimental values lie between those resulted from eqs. (3) and (4). Thus some interfacial adhesion exists and this is also quantified by the factor $B$, the adhesion parameter exhibited by a value greater than 1. The thermoplastic cellulose derivative (EC) and the compatibilizer enhanced the adhesion between the two phases.

Figure 7(a–d) shows the SEM micrographs of the tensile fractured surfaces for EVA–EC blend. The uncompatibilized blend with 20% EC loading exhibits its ductile fracture caused due to the shearing and crazing of the matrix and elongated voids seen due to cavitation of EC particles. All these absorb energy and give resistance fracture and this reflects in the high RTS value of 0.81 (Fig. 3). Addition of compatibilizer to the blend further enhances the [Fig. 7(b)] RTS value to 1.0 (Fig. 3), i.e., same as that of neat EVA. This shows that the matrix is able to withstand this filler loading and the two polar components (EVA and EC) show affinity to each even without the addition of an interfacial modifier.

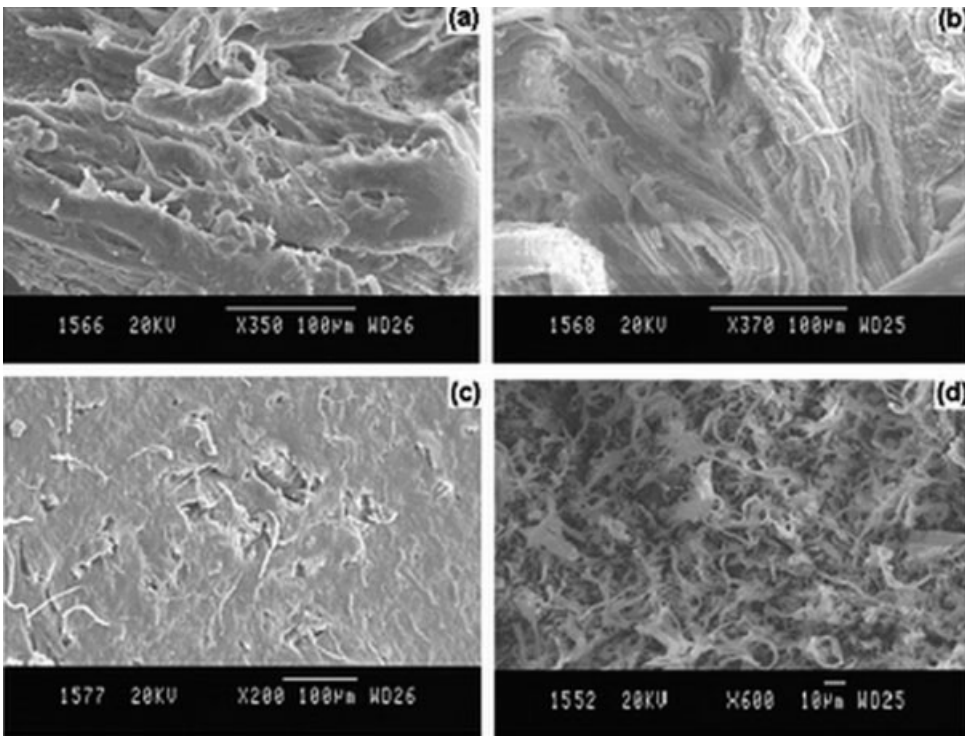


**Figure 7** SEM photographs showing tensile fractured blend specimens (a) blend containing 20% EC and no compatibilizer; (b) blend containing 20% EC and 6% compatibilizer; (c) blend containing 50% EC and no compatibilizer; and (d) blend containing 50% EC and 6% compatibilizer.

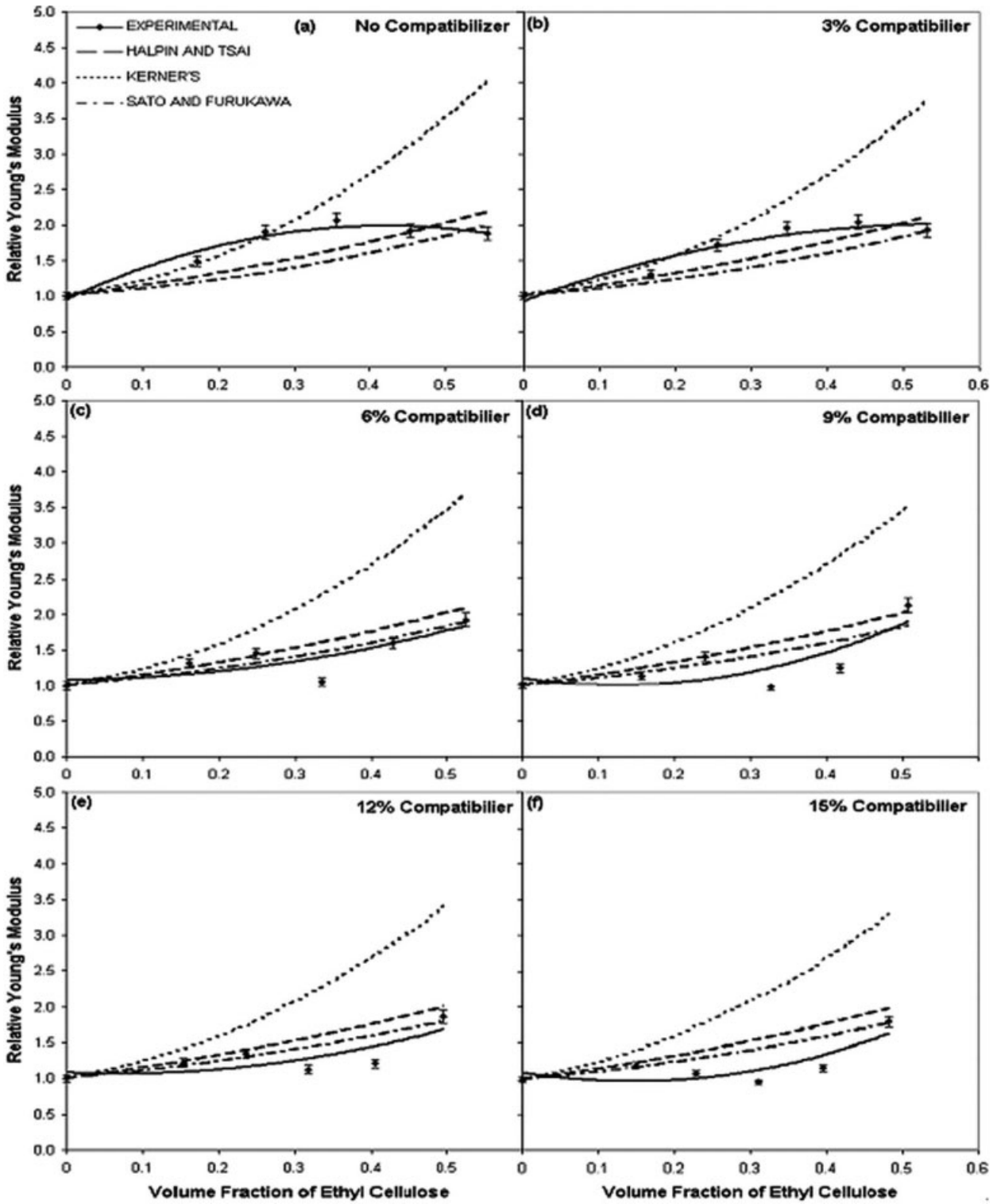


**Figure 8** Plot of RYM with volume fraction of EC for (a) no compatibilizer; (b) 3% compatibilizer; (c) 6% compatibilizer; (d) 9% compatibilizer; (e) 12% compatibilizer; and (f) 15% compatibilizer.

For a higher loading of 50% EC, the SEM micrograph shows predominantly brittle fracture [Fig. 7(c)] with large holes left by agglomerated EC particles. The rigid EC particles exhibits partial affinity toward polar EVA helps impart a high RTS value at par with neat EVA [Fig. 3(a)]. The compatibilized blend [Fig. 7(d)] shows quasi brittle fracture. The fracture surface is characterized by short fibrils accompanied by cavitation exhibiting a dimpled network. This occurs owing to better stress transfer

from matrix to filler and the RTS value is 1.26 (Fig. 3), i.e., even higher than neat EVA. Thus, EC behaves like reinforcing filler and the RTS values further increases on increasing the loading to 60% [Fig. 3(a)].

### Relative Young's modulus

Figure 8 shows the RYM versus volume fraction of the filler for EVA/EC blends. As the volume fraction of EC increases, the RYM value progressively increases due to the stiffening effect of EC chains. Compatibilization imparts flexibility owing to improved adhesion between filler and matrix.

Three theoretical models have been used to explain the experimental results. The first is Kerner's model[30] and is represented by the following eq. (8).

$$\mathrm{RYM} = \frac{E_b}{E_{\mathrm{EVA}}} = \left[1.0 + \left(\frac{\phi_f}{1-\phi_f}\right)\left(\frac{15(1-\upsilon)}{(8-10\upsilon)}\right)\right] \quad (8)$$

In eq. (8), $E_b$ and $E_{\mathrm{EVA}}$ are the tensile modulus of the blend and pure EVA, respectively. The value of Young's modulus of pure EVA obtained was 24.94 MPa. The $\langle r^2 \rangle$ value for the earlier eq. (8) is given in Table II. The experimental results do not match with the experimental results as the model assumes poor adhesion between filler and matrix shown in the Figure 8.

The second model is the Halpin-Tsai model[27] for RYM is given as follows.

$$\mathrm{RYM} = \frac{E_b}{E_{\mathrm{EVA}}} = \left[\frac{1 + G\eta_m\phi_f}{1 - \eta_m\phi_f}\right] \quad (9)$$

where,

$$\eta_m = \frac{R_m - 1}{R_m + G} \quad (10)$$

In the earlier equation, $R_m$ is the ratio of filler modulus to matrix modulus. The value of $R_m$ was determined by trial and error to match with the experimental results and this was found to be 4.5. The $\langle r^2 \rangle$ value for the earlier eq. (9) is given in Table II. The theoretical results thus calculated are also plotted in Figure 8. The model assumes perfect adhesion between matrix and filler. The obtained results are closer to the experimental results when compared with those obtained by Kerner's model.

The third model is the Sato-Furukawa model given[31,32] below in eq. (11).

$$\mathrm{RYM} = \frac{E_b}{E_{\mathrm{EVA}}} = \left[\left(1 + \frac{{\phi_f}^{2/3}}{2 - 2{\phi_f}^{1/3}}\right)(1 - \psi\xi t) - \frac{{\phi_f}^{2/3}\psi\xi}{\left(1 - {\phi_f}^{1/3}\right)\phi_f}\right] \quad (11)$$

where,

$$\psi = \left(\frac{\Phi_f}{3}\right)\left[\frac{1 + \phi_f^{1/3} - \phi_f^{2/3}}{1 - \phi_f^{1/3} + \phi_f^{2/3}}\right] \quad (12)$$

In eq. (11), $\xi$ is an adjustable parameter and its value depends on the extent of interfacial adhesion. The value of $\xi$ varies from 0 to 1.0 for perfect adhesion and no adhesion, respectively. For a $\xi$ value of 1.0, the adhesion is very poor leading to pullout of the matrix from the filler surface to create cavities around it. The $\xi$ value was obtained by trial and error to match with experimental results using FORTRAN program and was found to be 0.01 indicating very good interfacial adhesion. The result from this model has also been plotted in Figure 8. The $\langle r^2 \rangle$ value for the earlier eq. (11) is given in Table II. The theoretical results match well the experimental results.

It is obvious from the results that there exists a good interaction between EC and EVA as both are polar and thermoplastic. The ester groups of EVA can interact effectively with the ether group of EC. Furthermore, the compatibilizer can anchor itself with both the components leading to enhanced dispersion of EC in EVA. This results in better stress transfer from the matrix to filler leading to improved tensile properties.

### Relative elongation at break

Figure 9 shows the REB versus volume fraction of filler for EVA/EC blends. The REB values drop down drastically as the filler content increases. As the filler cannot deform, the matrix deformation is more leading to low REB values Nielsen's model[33] is the basic model for elongation at break and is given by,

$$\mathrm{REB} = \frac{\varepsilon_b}{\varepsilon_{\mathrm{EVA}}} = \left(1 - k\phi_f^{2/3}\right) \quad (13)$$

In eq. (13), $\varepsilon_b$ and $\varepsilon_{\mathrm{EVA}}$ are the elongation at break values for the blend and pure EVA, respectively. The value of elongation at break of pure EVA obtained was 158.8%. "$k$" is an adjustable parameter depending on filler geometry and is equal to 1.0 for perfect adhesion. The $\langle r^2 \rangle$ value for the earlier eq. (13) is given in Table II. For EVA/EC blends parameter was obtained by trial and error to match with the experimental values. The value of $k$ was found to be 0.7 indicating good adhesion between filler and matrix. The calculated theoretical values are also plotted in Figure 9. The REB experimental values are much lower than the predicted values for high EC loadings of 40–60%.

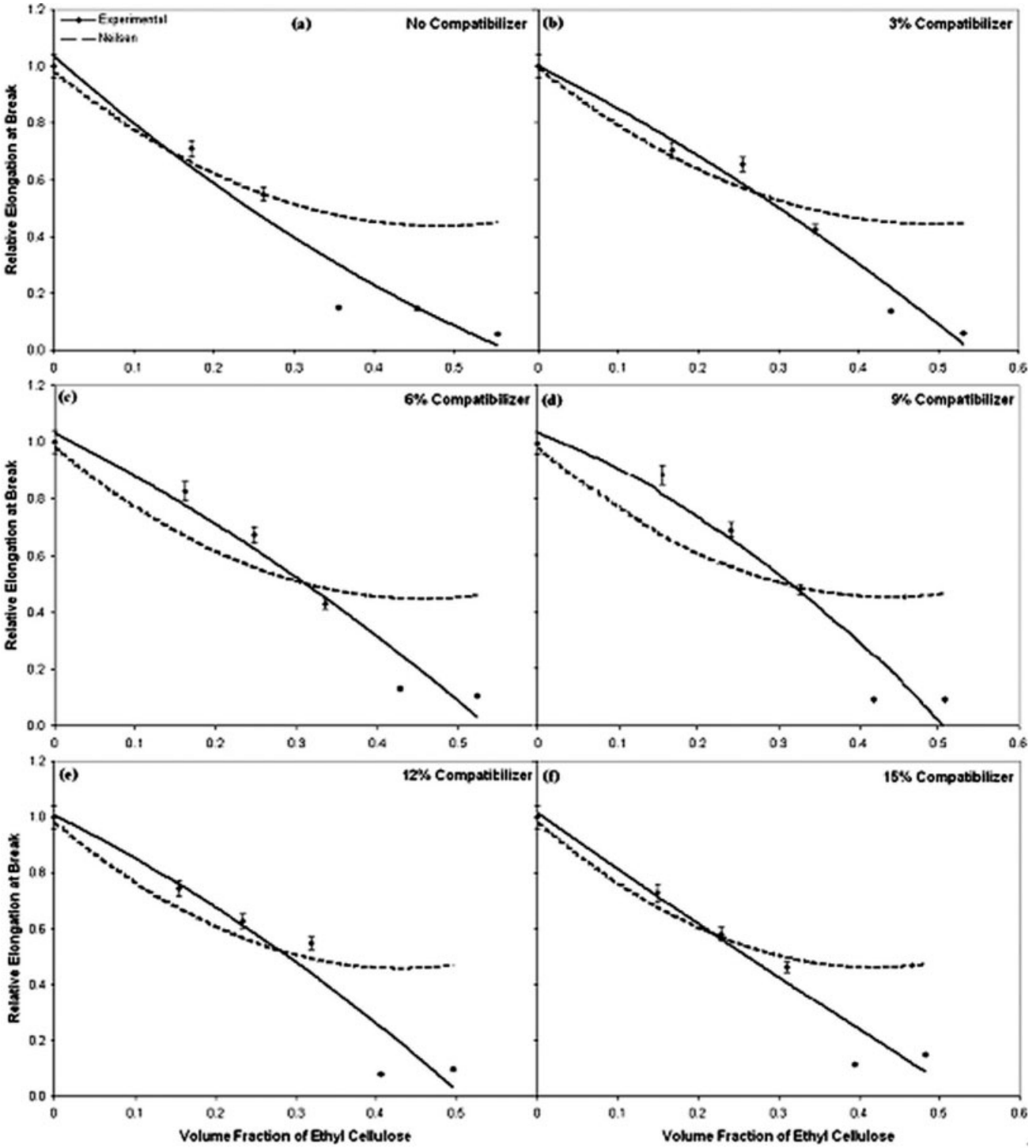


**Figure 9** Plot of REB with volume fraction of EC for (a) no compatibilizer; (b) 3% compatibilizer; (c) 6% compatibilizer; (d) 9% compatibilizer; (e) 12% compatibilizer; and (f) 15% compatibilizer.

### Thermogravimetric analysis (TGA)

Figure 10 shows the thermogravimetric analysis of EVA/EC blends. Curve (a) shows the thermal degradation for neat EVA. The onset of thermal degradation is at 313°C. The thermograms shows EVA undergoes two-stage degradation at 364°C (for vinyl acetate portion) and at 476°C (corresponding to 87% weight loss) due to the breakdown of ethylene chains. Ethyl cellulose has a maximum decomposition rate at 280°C.[34] The compatibilizer EVOH also has two peaks at 360°C and 414°C.[35] Thus, the peaks of EVOH have merged with those of EVA in the blends. For 40% EC loading (curve (b)), the two

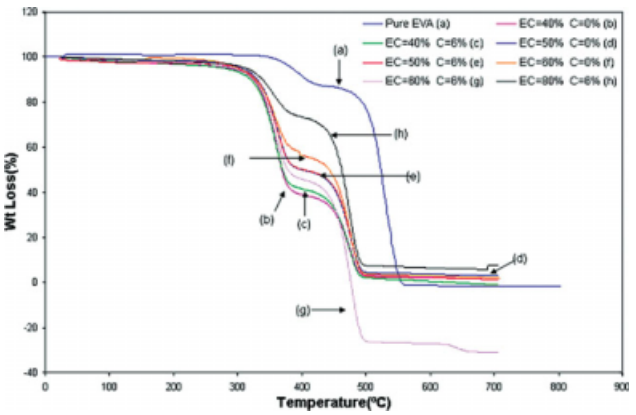


**Figure 10** Thermogravimetric analysis (TGA) of EVA/EC blends. [Color figure can be viewed in the online issue, which is available at www.interscience.wiley.com.]

peaks are shifted to a lower temperature. The same blend on compatibilization exhibits peak at the same temperatures (curve (c)) but the weight loss is higher owing to increased interactions. It may be that some part of EC is encapsulated by EVA and may undergo weight loss along with EC. For 50% (curves (d) and (e)) EC loading, the uncompatibilized and the compatibilized thermograms overlap with each other. The blends containing 60% EC (curves (f) and (g)) show a similar trend as that of 50% EC loading.

## CONCLUSIONS

The mechanical and thermal properties of biodegradable EVA/EC blends were examined by varying EC content from 0 to 60%. The hydrophobic EC chains had a reinforcing effect on the blend leading to high-tensile strength even with 50% EC loading. Compatibilization further improved the mechanical properties although the elongation at break reduced. All the blends exhibited optimal compatibilizer content due to saturation of reactive sites at the interface. TGA analysis showed a two-stage degradation and weight loss increased on compatibilization. The peak temperatures also shifted to lower values with increasing EC content.

## References

1. Mothe, C. G.; Tavares, M. I. B. Polym Degrad Stab 1997, 57, 183.
2. Vox, G.; Schettini, E. Polym Test 2007, 26, 639.
3. Briassoulis, D. Polym Degrad Stab 2006, 91, 1256.
4. Shyu, H.; Shyu, Y. U.S. Pat. 620,103,2B1, (2001).
5. Rosa, M. F.; Schiou, B.; Medeiros, E. S.; Wood, D. F.; Mattoso, L. H. C.; Oits, W. J.; Iman, S. H. 11th Annual NSTI Conference, Houston, USA, June 1–5, 2008.
6. Kim, M.; Lee, A.; Lee, K.; Chin, I.; Yoon, J. Eur Polym J 1999, 35, 1153.
7. Gassner, F.; Owen, A. J. Polymer 1992, 33, 2508.
8. Rimez, B.; Rahier, H.; Van Assche, G.; Artoos, T.; Biesemans, M.; Van Mele, B. Polym Degrad Stab 2008, 93, 800.
9. Yoon, J.; Oh, S.; Kim, M.; Chin, I.; Kin, Y. Polymer 1999, 40, 2303.
10. Gregory, C.; Laurent, H.; Rachid, A.; Karim, M. Biomacromolecules 2005, 6, 2025.
11. Soudis, Y.; Moga, L.; Blazek, J.; Lembot, R. J Anal Appl Pyrolysis 2007, 80, 36.
12. Prinos, J.; Bikiaris, D.; Theologidis, S.; Panayiotou, C. Polym Eng Sci 1998, 38, 954.
13. Sailaja, R. R. N.; Chanda, M. J Appl Polym Sci 2002, 86, 3126.
14. Senna, M. M.; Horsam, F. M. Polym Compos 2008, 29, 1137.
15. Malunka, M. E.; Luyt, A. S.; Krump, H. J Appl Polym Sci 2006, 100, 1607.
16. Yiking, H.; Xiaolie, L.; Dezhu, M. Eur Polym J 2001, 37, 2153.
17. Wu, C.; Huang, Y.; Chen, S. Polym Bull 2002, 48, 33.
18. Zhang, L.; Deng, X.; Huang, Z. Polymer 1997, 38, 5379.
19. Gonzlez, R.; Ramsay, F. J.; Favis, B. D. Polymer 2003, 44, 1517.
20. Lomellini, P.; Matos, M.; Favis, B. D. Polymer 1996, 37, 5689.
21. Sundararaj, U.; Macosko, C. W. Macromolecules 1995, 28, 2647.
22. Yamaoka, H. J Photopolym Sci Technol 2004, 17, 341.
23. Datt, S. C.; Singh, R.; Keller, J. M.; Khare, P. K.; Solanki, Y. Electrets, 1991. (ISE 7) Proceedings., 7th International Symposium on (Cat. No.91CH3029-6); 25–27 Sep 1991; Berlin, Germany.
24. Giunchedi, P.; Tore, M. L.; Maggi, L.; Conti, B.; Conte, U. J Microencapsul 1996, 13, 89.
25. Jiang, W.; Qiao, X.; Sun, K. Carbohydr Polym 2006, 65, 139.
26. Nicolais, L.; Narkis, M. Polym Eng Sci 1996, 17, 384.
27. Halpin, J. C.; Kardos, J. L. Polym Eng Sci 1976, 16, 344.
28. Miura, J.; Maeda, Y.; Machi, H.; Matsuda, S. Dent Traumatol 2007, 23, 9.
29. Turcsanyi, B.; Pukanszky, B.; Tudos, F. J Mater Sci Lett 1988, 7, 160.
30. Kerner, E. H. Proc Phys Soc 1956, 69, 808.
31. Sato, Y.; Furukawa, J. Rubber Chem Technol 1962, 35, 857.
32. Sato, Y.; Furukawa, J. Rubber Chem Technol 1963, 36, 1081.
33. Nielsen, L. E. J Appl Polym Sci 1966, 10, 97.
34. Aggour, Y. A. J Mater Sci 2000, 35, 1623.
35. Rosa, F.; Chiou, B.; Mederos, E. S.; Wood, D. F.; Mattoso, L. H. C.; Orts, W. J.; Imam, S. H. J Appl Polym Sci 2009, 111, 612.